Journal of Fluids and Structures (1992) **6**, 671–680

WAKE AND CAVITATION CHARACTERISTICS OF EQUILATERAL PRISMS AT INCIDENCE

R. BALACHANDAR AND A. S. RAMAMURTHY
Faculty of Engineering and Computer Science, Concordia University, 1455 de Maisonneuve Blvd. West, Montréal, H3G 1M8, Canada

(Received 3 April 1991 and in revised form 6 December 1991)

The characteristics of flow past a two-dimensional equilateral prism are experimentally studied at different angles of incidence to the approach flow. Tests were conducted in a water tunnel suitable for cavitation studies. The presence of cavitation facilitated excellent visual observations of the wake region. The mean separation pressure coefficients and the vortex-shedding frequency were determined at various degrees of cavitation for five different orientations of the prism. The latter determines, to a large extent, the vibration characteristics of the system in which the prismatic elements are located.

1. INTRODUCTION

FLOW PAST BLUFF BODIES has been studied quite extensively, and a significant body of knowledge has been gathered in the last two decades. Flow fields which have received the most attention include two-dimensional flow past circular cylinders, normal flat plates, prisms, square sections and axisymmetric bodies with various head-forms. The cross-sectional shape of the body largely determines the position of the separation points and hence the hydrodynamic characteristics of the flow. In the case of sharp-edged bluff bodies, the position of the separation points is fixed and thus provides definite control points to analyse the flow field. On the other hand, for flow past two-dimensional circular cylinders, the location of the separation points shifts with Reynolds number. This shift results in the hydrodynamic characteristics like drag coefficient and Strouhal number to be highly dependent on the Reynolds number, especially in the critical Reynolds number range of flow. In practice, due to ease of construction and economy, sharp-edged structures are often used as hydraulic elements. In a recent review, Knisely (1990) has pointed out that situations do arise where a structural member may be oriented to the flow direction at different angles of incidence. In the field, some of these structures are subject to undesirable cavitation effects. Flow past flat plates at different angles of incidence has been studied by Abernathy (1962) and Shaw (1971) under non-cavitating conditions. Abernathy (1962) obtained the pressure distribution around the plate and the vortex-shedding frequency for three different incidences to the approach flow. Grant *et al.* (1981) measured the vortex-shedding frequency as a function of the angle of attack for L- and T-section beams. They observed two distinct values of Strouhal numbers, with the change from one value to the other occurring for a small change of angle of incidence.

Cavitating flow past bluff bodies has also been studied quite extensively in the past (Waid 1957; Ramamurthy 1977). Some discrepancies in the hydrodynamic characteristics have been noted in the case of flow past cavitating circular cylinders. Such discrepancies are generally a consequence of the shift in separation points with varying Reynolds numbers. Studies into characteristics of cavitating flow past bluff bodies with

0889–9746/92/060671 + 10 $08.00

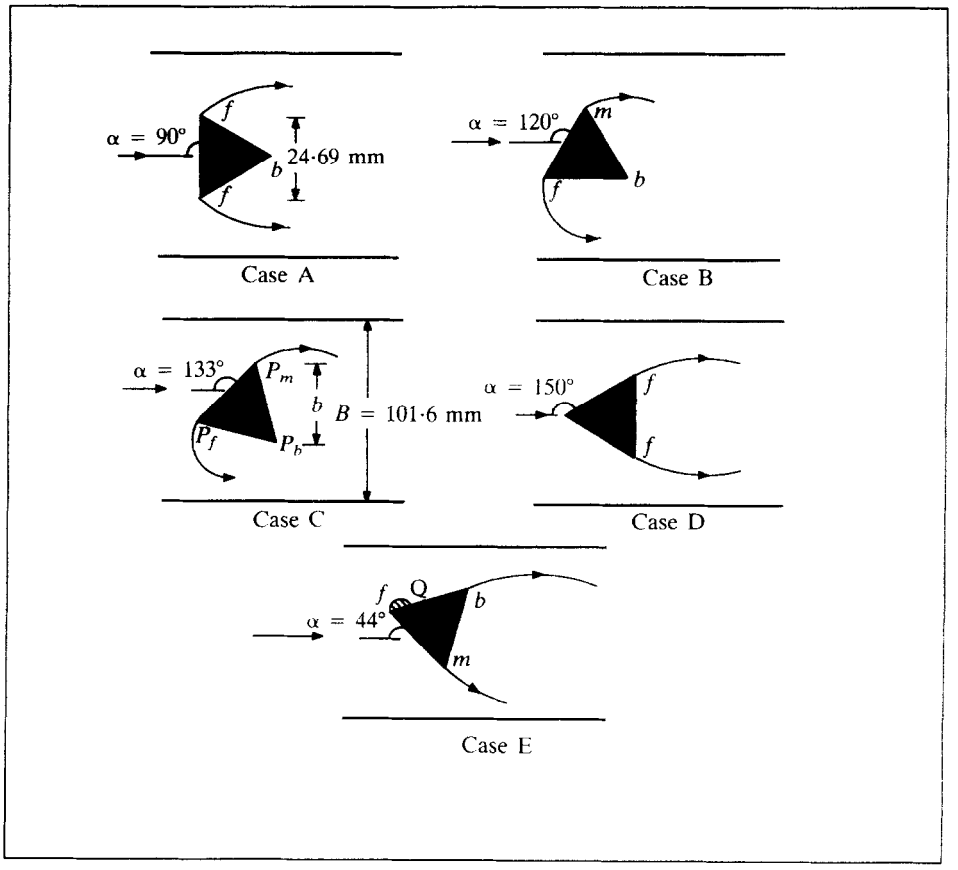

Figure 1. Flow past an equilaternal prism at different angles of incidence.

fixed separation points have also been carried out in the past (Young 1966; Bhaskaran 1977). Most of the bodies studied have a physically unrestricted wake downstream of the separation points. Sarpkaya (1961) has conducted a detailed study of the cavitation characteristics of butterfly valves at various angles of incidence. The effect of blockage on the cavitation characteristics of bluff bodies has also been studied recently by Balachandar (1990).

In the present study, a sharp-edged equiangular prism formed the basic test body. The body was tested under five different orientations (Figure 1). Though the wake formed behind each orientation of the body was physically unrestricted, the wake geometry was distinct for each case. In some instances, the test body would by symmetrical to the approach flow, and at other orientations the wake formed would be asymmetrical. For all orientations of the body, a well-defined Karman vortex street was formed in the wake. The presence of cavitation aided visual observation of the wake region. The frequency of vortex shedding and the pressures at separation were obtained under various cavitating conditions.

2. EXPERIMENTAL SET-UP AND PROCEDURES

The water tunnel used in the study has a 10:1 contraction preceding the test section and yielded a nearly uniform velocity at the test section. The test section was 101·6 mm high, 50·8 mm wide and 508 mm long (Figure 2) and had plexiglas windows to facilitate

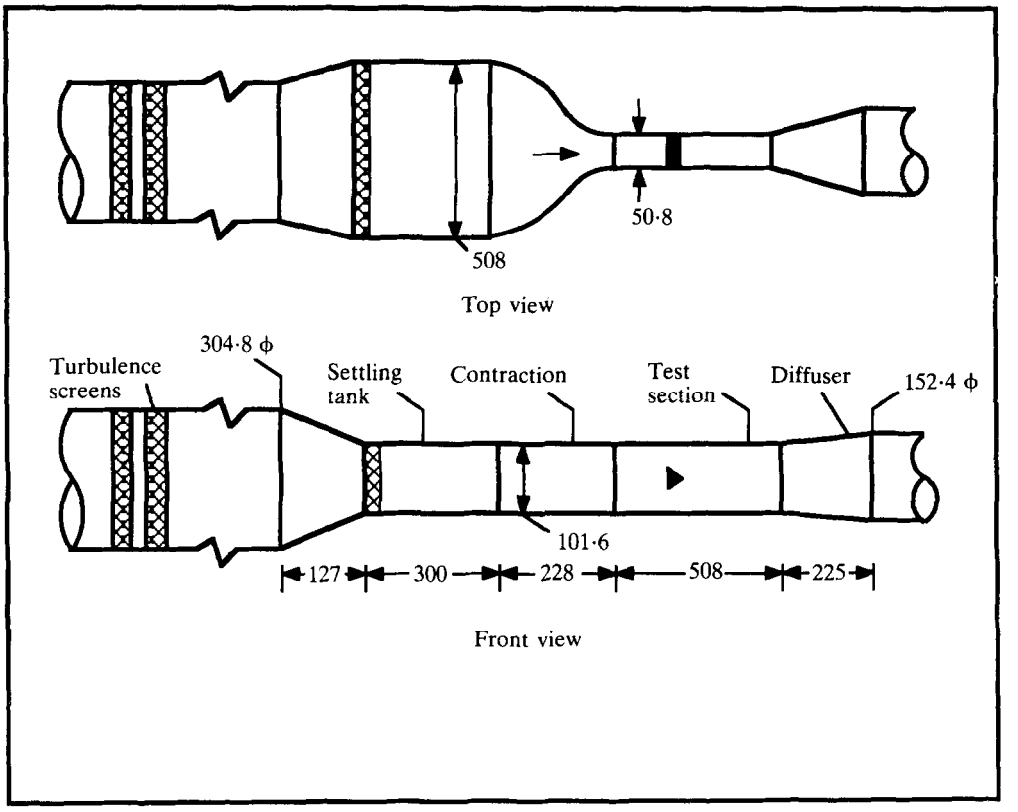

Figure 2. Schematic of the water tunnel used in the experiments (not to scale); all dimensions in mm.

visual observations. Experiments were carried out to check the quality of flow in the unobstructed test section. Span-wise uniformity checks of the axial velocity distributions were made at a section 50 mm downstream from the inlet, in horizontal planes perpendicular to the flow, using a 15 mW dual beam He–Ne Laser Doppler velocimeter (TSI Inc.) in the forward scatter mode. The span-wise velocities were found to be uniform to within 3% over the middle 80% of the span. Furthermore, the ratio of the test section average velocity to the centre-line velocity was of the order of 0·94. These are indicative of the two-dimensional nature of flow in the test section. A mass balance check was also conducted over the entire test section assuming two-dimensional flow. The mass balance checked to within 3%. Several turbulence-reducing honeycombs were placed ahead of the contracting section. The turbulence levels in the test section were of the order of 1%.

A polished equilateral brass prism of side 24·69 mm formed the basic test body. The test body was 50·8 mm wide and spanned the entire test section. The orientation, α (Figure 1) refers to the angle of incidence of the flow measured in the clockwise direction. The five orientations of the test body are denoted as case A, B, C, D and E, respectively. Test cases B, C and E are asymetrical to the approach flow. The cases reported by previous studies (Young & Holl 1966; Balachandar 1990; Bhaskaran 1977) generally refer to symmetrical flow situations. Cases A and D not only provided additional data about also served to calibrate the present test facility and experimental procedures adopted. A pressure tap 0·5 mm in diameter was located at the centre of the front face of the body to measure the stagnation pressure for the case $\alpha = 90°$ The

pressures at the corners (P_f and P_m, Case C, Figure 1) were measured by means of pressure taps located 1 mm downstream of the separating edges, as opposed to being placed at the edges themselves. This was found necessary from earlier experience (Balachandar 1990) to avoid the influence of the tap on the separating streamline. Using calibrated pressure gauges, the positive pressures were measured to the nearest 1·72 kPa, while the negative pressures were measured to the nearest 6·35 mm of mercury. The freestream pressure ranged from 0 to 70 kPa, while the test-section velocity ranged from 3 to 9 m/s. During each test run, the water temperature was noted to the nearest 0·25°C. During the test series, the temperature ranged from 22 to 24°C and the air content from 9 to 11 ppm. However, during any specific run, the change in air content was negligibly small. The flow was measured with the help of a standard 60° V-notch. The depth of flow over the notch was measured to the nearest 0·10 mm and the accuracy of discharge measurement is estimated to be 3%.

In the present study, the maximum solid blockage was 24·3%. As the model was rotated the blockage was slightly altered. To avoid using multiple bodies and limit errors in measurements, a single body was chosen. This necessitated a higher degree of blockage in order to enable one to conduct tests at various degrees of cavitation including choking conditions. Furthermore, a better visualization of flow separation and vortex-shedding process was obtained at a higher blockage (Balachandar 1990). No attempts were made to repeat the tests at other blockages, since the effect of blockage has been reported earlier (Bhaskaran 1977). In the present study, it should be noted that for four of the orientations of the prism (Cases A to D), the flow is characterized by two separation points (Figure 1). Case E is characterized by separation at all three vertices of the body. The presence of cavitation in the core of the vortices aided the flow visualization process.

The presence of imperfections, such as microbubbles in the water, influences the scaling laws. These imperfections are commonly denoted as cavitation nuclei and contain vapour, undissolved gas or both. The inception of cavitation is associated with the growth of these nuclei. Qualitative relationships between cavitation inception and nuclei have been developed by Holl (1970). As rightly pointed out by Blake (1986), beyond a rather notional relationship between nucleus population and cavitation, there is no rigorous theory in hydrodynamic cavitation that satisfactorily explains or accounts for the influence of nuclei in a quantitative sense. In the present series of tests, it should be noted that the size and shape of the test body chosen was such that the inception cavitation indices were reasonably high. It is expected that the characteristics of nuclei and dissolved gas effects may not have a significant effect on the test results (Arakeri 1981; Balachandar 1990). Further, no efforts were made to obtain the inception cavitation indices at different orientations. Nevertheless, to determine the characteristics of nuclei in water, a Laser particle dynamic analyser (Dantec Inc.) was used to record the stream nuclei in the range 0–100 μm (Ramamurthy 1991). Test data indicated that the mean diameter of the particles in water ranged from 14 to 20 μm and did not vary over a range of velocities.

The frequency of pressure pulsations in the wake was obtained with the help of pressure transducers located on the tunnel wall close to the edge of the free shear layer. The output signal from the transducer demodulator was fed to a Fast Fourier Transform Analyser (Wavetek, 5830-A) to carry out the spectral analysis. A stroboscope (Brüel and Kjaer, Type 4912) and a battery of powerful lights aided visual observation. During any given test run, to enable visual observations, the internal generator of the stroboscope was manually set at the vortex-shedding frequency "f" determined from the spectral measurements. Based on the vapor pressure, P_v, the

cavitation number σ is defined as follows:

$$\sigma = \frac{P - P_v}{\frac{1}{2}\rho U^2}, \tag{1}$$

where P and U are the freestream pressure and velocity, respectively, and ρ is the density of water. The following pressure coefficients are also defined:

$$C_{pf} = \frac{P_f - P}{\frac{1}{2}\rho U^2}, \qquad C_{pb} = \frac{P_b - P}{\frac{1}{2}\rho U^2} \quad \text{and} \quad C_{pm} = \frac{P_m - P}{\frac{1}{2}\rho U^2}, \tag{2}$$

where P_f refers to the steady pressure at the leading separation point, P_b to the steady pressure at the rear-most point of the body, and P_m to the steady pressure at the intermediate edge of the body. These pressures are measured to obtain an estimate of the steady forces acting on the test body at different orientations. For clarity, these pressures are identified for the orientation of Case C in Figure 1. In terms of the frequency of vortex shedding, f, the Strouhal number is defined as

$$S = \frac{fb}{U}, \tag{3}$$

where b refers to the projected chord of the test body perpendicular to the approach flow (Case C, Figure 1). In the forthcoming results, the discrepancy in the reported values of the σ, S and the pressure coefficients is estimated to be of the order of $\pm 0{\cdot}03$, $\pm 0{\cdot}005$ and $\pm 0{\cdot}03$, respectively.

3. ANALYSIS OF RESULTS

3.1. Pressures at Leading Edge Separation

Figure 3 shows the variation of the leading edge separation pressure coefficient, C_{pf}, with, σ, for all the orientations tested. Case A being the most bluff, has the smallest values of C_{pf} at the larger values of σ. The variation of C_{pf} with σ show similar trends for cases A and D. In both the cases, as the value of σ is reduced from non-cavitating values (large σ), the values of C_{pf} increase. It should be noted that for all orientations denoted in Figure 1, the flow in the wake is dominated by the presence of an alternate vortex-shedding mechanism and the formation of the well-known Karman vortex street. For Case A and Case D, the velocities and hence the pressures are the same at both points of separation. In particular, for Case D, the pressure is constant along the rear of the body. One notes from Figure 3, that the variation of C_{pf} with σ shows a slightly different trend for Cases B and C when compared to Case A. As the value of σ is reduced from a non-cavitating value, C_{pf} remains constant up to a value of around 6. Beyond this, C_{pf} values first decrease and then increase with decreasing σ. At lower values of σ, the data appear to merge with those of Case A. In fact, at very low values of σ, as choking conditions are approached, the cavity region appears foamy and the pressures at separation approach the vapor pressure. Consequently, $P_f \simeq P_v$ and, hence, the values of C_{pf} for all orientations are expected to have the same trend at very low values of σ. It should be noted that for all the cases tested, the pressure coefficient, C_{pf}, refers to the measurements at the leading separation point closest to the stagnation point on the forebody. For cases A to D, there is a large-scale separation and vortex shedding from this edge of the body. However, for Case E, visual observations indicate the presence of a local separation at the point of measurement of

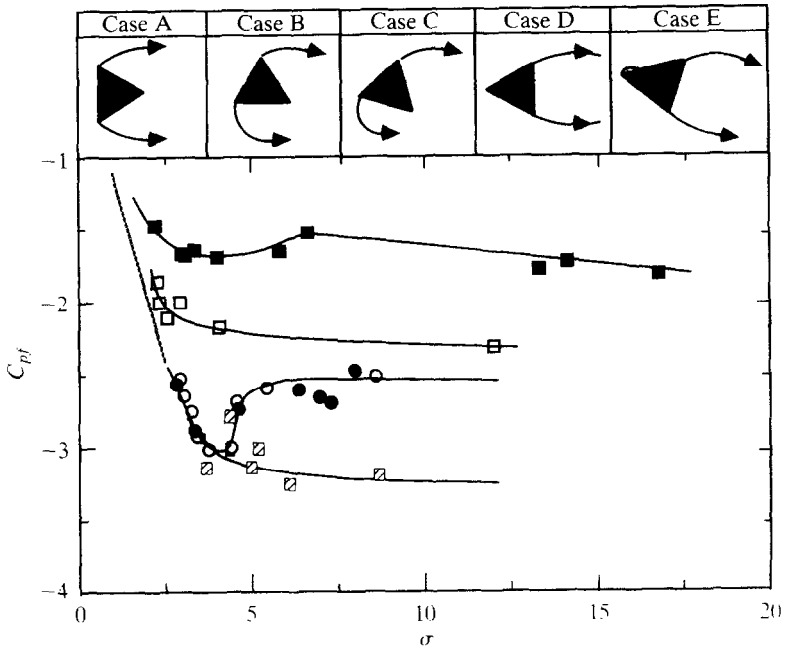

Figure 3. Variation of leading-edge separation pressure coefficient, C_{pf}, with the cavitation number, σ. ▨, Case A; ○, Case B; ●, Case C; □, Case D; ■, Case E.

P_f and subsequent reattachment at Q (Case E, Figure 1). The values of C_{pf} are significantly higher at all values of σ for Case E when compared to other orientations of the body.

3.2. Pressures at the Rear Tip and Intermediate Edge of the Body

Figure 4 shows the variation of C_{pb} with σ for all five orientations of the test body. For Case A, the presence of the afterbody of the wedge causes the pressures to drop below

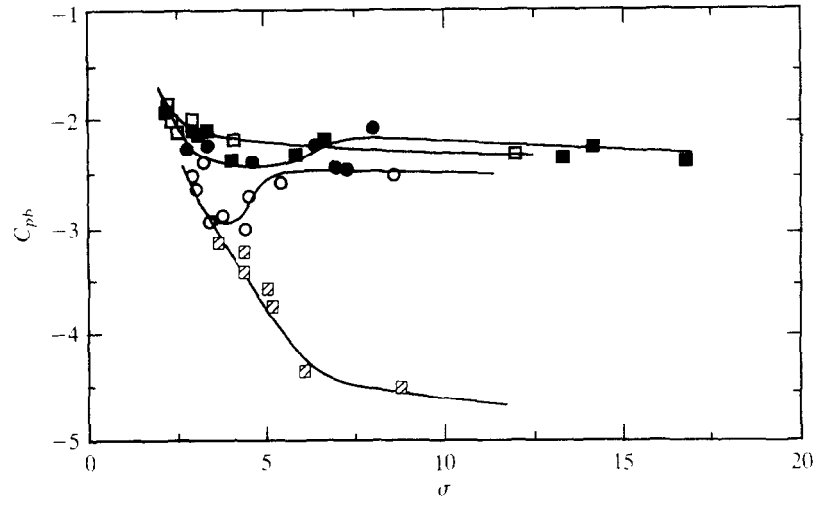

Figure 4. Variation of the back pressure coefficient, C_{pb}, with σ. ▨, Case A; ○, Case B; ●, Case C; □, Case D; ■, Case E.

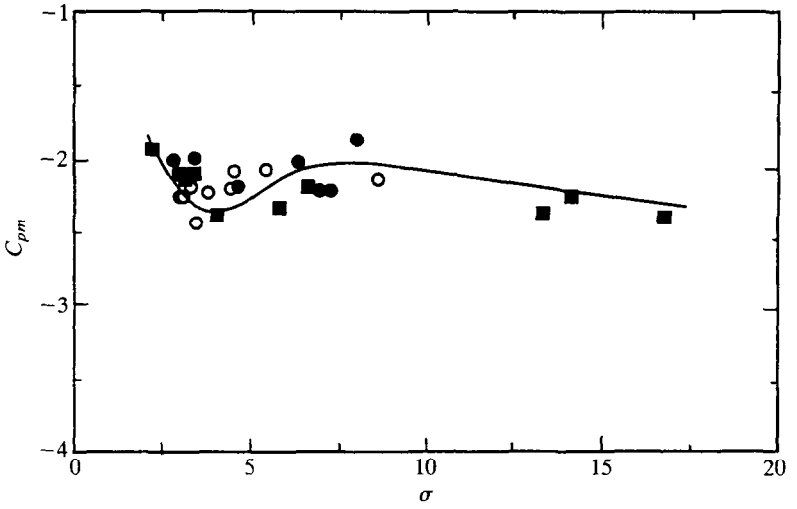

Figure 5. Variation of the intermediate-edge separation pressure coefficient, C_{pm}, with σ. ○, Case B; ●, Case C; ■.

those at separation. A similar behaviour has been noticed earlier by Ramamurthy & Lee (1973) in noncavitating flows and by Ramamurthy & Bhaskaran (1977) in cavitating flows. The data for Case D and Case E are very similar, in view of the large-scale vortex shedding from this edge. For Case B, the values of C_{pb} follow a trend similar to that of C_{pf}. Figure 5 shows the pressure distribution occurring at the intermediate edge of the body for Case B, C and E. The data appear to have a similar trend for all the three cases. The measured pressure coefficients indicate that the orientation to the approach flow has a large influence on the overall forces acting on the body. The pressures at the corners of the test body are not equal, especially for the

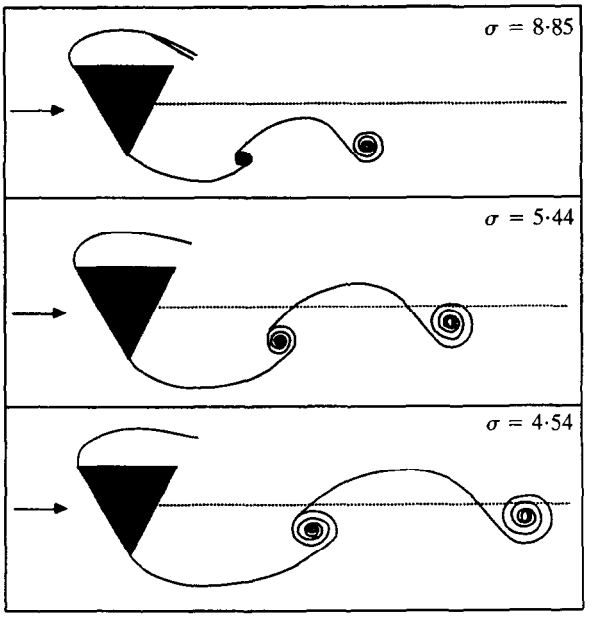

Figure 6. Schematic of the flow field for Case B (see Figure 1).

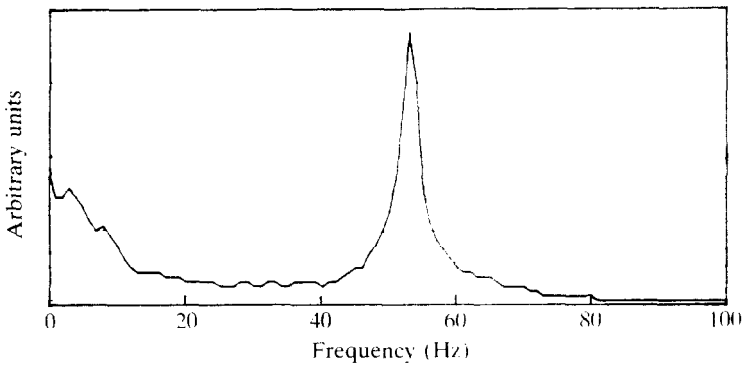

Figure 7. Typical power spectrum of pressure fluctuations, for Case B, $\sigma = 8{\cdot}58$.

asymetrical cases. Further, the pressures over the entire cavity tend to be uniform only for those values of σ corresponding to choking conditions.

3.3. Vortex-shedding Process

The presence of cavitation facilitates visual observation of the wake region. During such observations, large-scale vortex formations were clearly discernible in the wake. Figure 6 qualitatively shows a schematic of the flow field observed for Case B at different degrees of cavitation. Figure 7 shows a typical power spectrum of pressure fluctuations occuring in the wake. The pressure records and the corresponding frequencies were obtained at several locations in the wake. The dominant frequency and the general shape of the spectra remained the same at any particular cavitation number for all locations of the transducer. Using these frequencies and equation (3), one can obtain the Strouhal numbers at various cavitation conditions. Figure 8 shows the variation of S with σ for all orientations spanning noncavitating to choking conditions. A decrease in σ from noncavitating conditions results in little or no change in the value of S until a certain cavitation number is reached. Similar observations have been recorded earlier (Balachandar 1990; Ramamurthy 1977; Young 1966) for

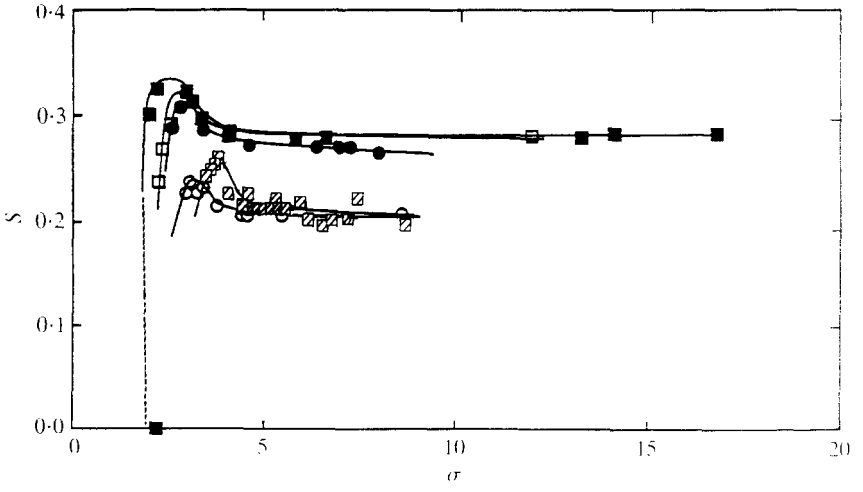

Figure 8. Variation of Strouhal number, S, with the cavitation number, σ, for all orientations studied. ▨, Case A; ○, Case B; ●, Case C; □, Case D; ■, Case E.

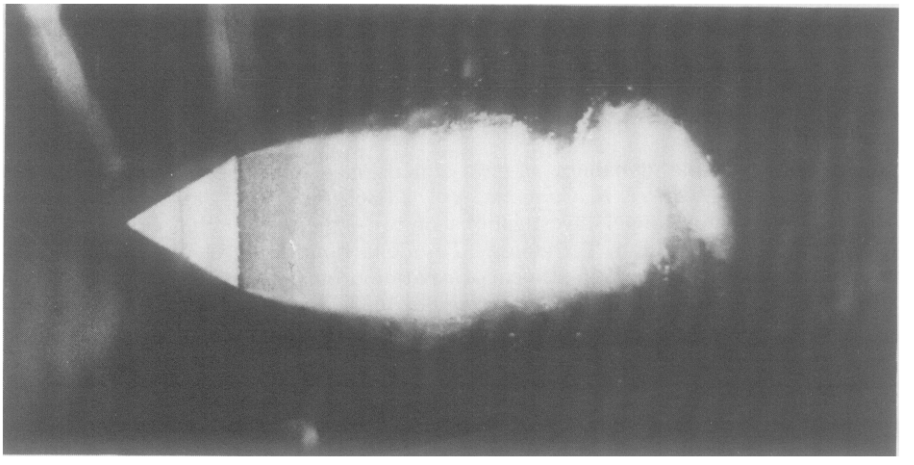

Figure 9. Typical photograph of wake region near choking conditions (Case D, Figure 1).

symmetrical flow situations. With a further decrease in cavitation number, the Strouhal number increases, reaches a maximum and decreases further as choking conditions are approached. The vortex shedding becomes highly intermittent, just prior to choking. At very low cavitation numbers, the spectra of pressure fluctuations do not indicate a clear dominant frequency. Figure 9 shows a photograph taken near choking conditions for Case D. It shows the formation of the vortex at the tip of the cavity. In fact, the formation of this vortex occurs intermittently. Interestingly, Cases C, D and E quantitatively show a very similar variation in Figure 8, inspite of the differing incidence to the approach flow.

4. CONCLUSIONS

As the angle of incidence of the equilateral prism to the approach flow is altered, the vortex-shedding frequency and the pressure distributions around the body are altered. At any given orientation, cavitation has a significant influence on the flow characteristics. The presence of cavitation facilitated excellent visual observations of the wake region.

References

Abernathy, F. H. 1962 Flow over an inclined flat plate. *ASME Journal of Basic Engineering* **84,** 380–388.

Arakeri, V. H. 1981 Inception of cavitation from a backward facing step. *ASME Journal of Fluids Engineering* **103,** 288–293.

Balachandar, R. 1990 Characteristics of separated flows including cavitation effects. Ph.D Thesis, Concordia University, Montréal, Canada.

Bhaskaran, P. 1977 Characteristics of cavitating flow past bluff bodies. Ph.D Thesis, Concordia University, Montréal, Canada.

Blake, W. K. 1986 *Flow induced sound and vibration,* Vol. 1. London: Academic Press Inc.

Grant, I. & Barnes, F. H. 1981 The vortex shedding and drag associated with structural angles. *Journal of Wind Engineering and Industrial Aerodynamics* **8,** 115–122.

Holl, J. W. 1970 Nuclei and Cavitation. *ASME Journal of Basic Engineering* **92,** 681–688.

Knisely, C. W. 1990 Strouhal numbers of rectangular cylinders at incidence: A review and new data. *Journal of Fluids and Structures* **4,** 371–393.

Ramamurthy, A. S. & Lee, P. M. 1973 Wall effects on flow past bluff bodies. *Journal of Sound and Vibration* **31,** 443–451.

RAMAMURTHY, A. S. & BHASKARAN, P. 1977 Constrained flow past cavitating bluff bodies. *ASME Journal of Fluids Engineering* **99,** 717–726.

RAMAMURTHY, A. S. & BALACHANDAR, R. 1991 Flow past backward facing steps including cavitation effects. *ASME Journal of Fluids Engineering* **113,** 278–284.

SARPKAYA, T. 1961 Torque and cavitation characteristics of butterfly valves. *Journal of Applied Mechanics* **29,** 511–518.

SHAW, T. L. 1971 Wake dynamics of two-dimensional structures in confined flows. In *Proceedings of 14th I. A. H. R. Congress*, Vol. 2, B6, pp. 43–48, Paris. Delft: IAHR.

WAID, R. L. 1957 Water tunnel investigations of two-dimensional bluff bodies. Report No. E-73.6, California Institute of Technology, Pasadena, California, U.S.A.

YOUNG, J. O. & HOLL, J. W. 1966 Effects of cavitation on periodic wakes behind symmetric wedges. *ASME Journal of Basic Engineering* **88,** 163–176.

APPENDIX: NOMENCLATURE

b	projected chord of test body
B	width of test section
C_{ph}	back pressure coefficient
C_{pf}	leading-edge separation pressure coefficient
C_{pm}	intermediate-edge separation pressure coefficient
f	frequency of pressure pulsations
P	freestream pressure
P_b	back pressure
P_f	leading edge separating pressure
P_m	intermediate edge separation pressure
P_v	vapor pressure
ppm	parts per million
S	Strouhal number
U	approach velocity
σ	cavitation number